The Astronomical Journal, 153:225 (10pp), 2017 May https://doi.org/10.3847/1538-3881/aa67f6

The Curious Case of PDS 11: A Nearby, >10 Myr Old, Classical T Tauri Binary System

Blesson Mathew[1], P. Manoj[1], B. C. Bhatt[2], D. K. Sahu[2], G. Maheswar[3], and S. Muneer[2]
[1] Department of Astronomy and Astrophysics, Tata Institute of Fundamental Research, Colaba, Mumbai 400005, India; blesson.mathew@tifr.res.in
[2] Indian Institute of Astrophysics, Koramangala, Bangalore 560034, India
[3] Aryabhatta Research Institute of Observational Sciences (ARIES), Nainital 263002, India
Received 2016 November 7; revised 2017 March 16; accepted 2017 March 16; published 2017 April 24

Abstract

We present results of our study of the PDS 11 binary system, which belongs to a rare class of isolated, high Galactic latitude T Tauri stars. Our spectroscopic analysis reveals that PDS 11 is an M2–M2 binary system with both components showing similar Hα emission strengths. Both the components appear to be accreting and are classical T Tauri stars. The lithium doublet Li I λ6708, a signature of youth, is present in the spectrum of PDS 11A, but not in PDS 11B. From the application of lithium depletion boundary age-dating method and a comparison with the Li I λ6708 equivalent width distribution of moving groups, we estimated an age of 10–15 Myr for PDS 11A. Comparison with pre-main sequence evolutionary models indicates that PDS 11A is a 0.4 $M_{\odot}$ T Tauri star at a distance of 114–131 pc. PDS 11 system does not appear to be associated with any known star-forming regions or moving groups. PDS 11 is a new addition, after TWA 30 and LDS 5606, to the interesting class of old, dusty, wide binary classical T Tauri systems in which both components are actively accreting.

Key words: binaries: general – circumstellar matter – infrared: stars – stars: low-mass – stars: pre-main sequence – stars: variables: T Tauri, Herbig Ae/Be

1. Introduction

T Tauri stars are low-mass (K and M spectral types) young stars that are in their pre-main sequence phase of evolution (e.g., Joy 1945; Bertout 1989; Herczeg & Hillenbrand 2014). They are often associated with cloud complexes such as Taurus, Orion, and Ophiuchus (Herbig 1962; Appenzeller & Mundt 1989; Herczeg & Hillenbrand 2014). However, T Tauri stars are also found in isolated regions above the Galactic plane and far from any dark clouds (de la Reza et al. 1989; McGehee 2008; Elliott et al. 2016). TW Hydrae was the first such "isolated T Tauri star" identified, which was later found to be part of an association of about three dozen members, known as TW Hydrae association (TWA; Kastner et al. 1997; Zuckerman & Song 2004; Mamajek 2016). They were not runaway stars from molecular clouds, but formed in situ in the present region ~10 Myr ago, which is now devoid of molecular gas (Rucinski & Krautter 1983; Tachihara et al. 2009). Since then, several such nearby young associations have been identified, such as the β Pictoris moving group, the AB Doradus moving group, the Tucana/Horologium association etc., within 100 pc of the Sun (see Zuckerman & Song 2004; Torres et al. 2008; Mamajek 2016, for a review).

In this paper, we present a detailed analysis of the high Galactic latitude ($b = -30°$) binary T Tauri star system PDS 11 (GSC 04744-01367, IRAS 04451-0539). Gregorio-Hetem et al. (1992) have reported this to be a binary system with components of the Pico dos Dias Survey (PDS) 11A and PDS 11B. PDS 11A is the northeastern component of the binary (Figure 1). PDS 11A and PDS 11B are present in the Washington double star (WDS) catalog, with the component magnitudes being 14.76 and 15.34, respectively. The position angle (PA) and separation were found to be 216° and 8.″8, respectively (Mason et al. 2001). Our analysis indicates that PDS 11 is a young (10–15 Myr), nearby (114–131 pc) binary T Tauri system, where both the components are possibly accreting. The paper is arranged as follows. Section 2 describes the optical and near-IR observations. The results from this study are presented in Section 3. A detailed discussion of the key results is given in Section 4. Finally, in Section 5 we present our conclusions.

2. Observations and Data Reduction

2.1. Optical Spectroscopy

Optical spectra of both the components of the PDS 11 system in the wavelength range 3800–9000 Å were obtained with the Himalayan Faint Object Spectrograph Camera (HFOSC)[4] mounted on the 2 m Himalayan Chandra Telescope (HCT). The wavelength range was covered using Grism 7 (blue region, 3800–5500 Å) and Grism 8 (red region, 5500–9000 Å). The grisms in combination with 1.″92 wide and 11′ long slit provide an effective resolving power of ~900 in the blue region and ~1050 in the red region. A spectrophotometric standard, Feige 34, was observed on the same night and is used for flux calibration. The observations were carried out on 2016 February 13. The FeNe, FeAr lamp spectra were taken after each on-source exposure for wavelength calibration. The spectra were reduced in a standard manner after bias subtraction and flat-field correction using the standard tasks in Image Reduction and Analysis Facility (IRAF).[5] Furthermore, the extracted spectra were wavelength calibrated and flux calibrated. The target was again observed on March 15 to confirm the spectral features observed. The log of observations is given in Table 1.

[4] Further details of the instruments and telescopes is available at http://www.iiap.res.in/iao/hfosc.html
[5] IRAF is distributed by the National Optical Astronomy Observatories, which are operated by the Association of Universities for Research in Astronomy, Inc., under cooperative agreement with the National Science Foundation.

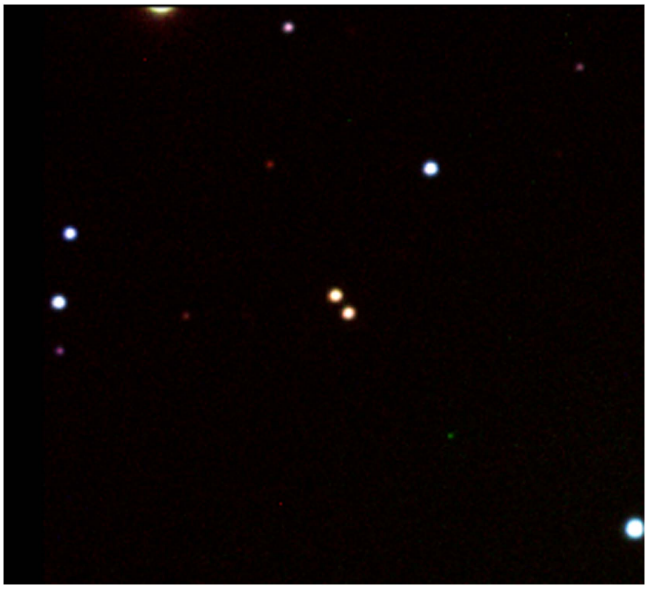

Figure 1. *BVR* color composite of PDS 11, with north up and east to the left. This $4' \times 4'$ composite image is constructed from our observations with the HCT and is color coded as blue, green, and red in *B*, *V*, and *R*, respectively. The image is centered on PDS 11 binary system, with the northeastern component being PDS 11A.

2.2. Near-infrared Spectroscopy

We also obtained near-IR spectra of PDS 11 with the TIFR near-infrared spectrometer and imager (TIRSPEC; Ninan et al. 2014) mounted on 2 m HCT. The spectra were taken in *Y* (1.02–1.20 μm), *J* (1.21–1.48 μm), *H* (1.49–1.78 μm), and *K* (2.04–2.35 μm) bands, in combination with Grism and L3 slit ($1\farcs97$ wide and $300''$ long). The effective resolving power is around 1200. The program stars PDS 11A and PDS 11B are co-aligned in the slit, and care is taken while reducing the spectra to extract them separately. A telluric standard HIP 34768 (A1V spectral type) at nearby airmass was also observed. The observations were carried out in dithered mode. The log of infrared spectroscopic observations is given in Table 1. Argon spectra were obtained after the object spectra for wavelength calibration. The wavelength calibrated object spectrum is divided with the the telluric spectrum whose hydrogen absorption lines were removed. The resultant spectrum is multiplied with a blackbody spectrum of 9230 K, corresponding to A1V spectral type of the telluric standard (Kenyon & Hartmann 1995). The final spectrum is normalized with respect to the band center in *Y*, *J*, *H*, and *K* bands.

2.3. Optical Photometry

We imaged the $10' \times 10'$ region centered on PDS 11 in *BVR* passbands (Bessell 1990) on 2016 March 19 using HFOSC. The data reduction was carried out using various packages available in IRAF. Aperture photometry was performed on the program star and nearby field stars. The *B*, *V*, and *R* magnitudes of the nearby field stars were obtained using available SDSS photometry, which were converted to Bessell system using the transformation relations.[6] The magnitude of the program stars were calibrated differentially with respect to the nearby field stars.

[6] https://www.sdss3.org/dr10/algorithms/sdssUBVRITransform.php

3. Results

3.1. Spectral Analysis: Optical and Near-IR

The spectra of both PDS 11A (Figure 2) and PDS 11B (Figure 3) look very similar due to the presence of Balmer emission lines, from Hα all the way up to H8 (8–2), Ca II H and K emission lines and TiO absorption bands, albeit with different line strengths. Gregorio-Hetem et al. (1992) reported an Hα equivalent width (EW) of -20 Å for PDS 11A and -42 Å for PDS 11B. The equivalent width measured from our spectra are -23 Å and -27 Å, which is quite different from the earlier measurements, particularly for PDS 11B. The EW and full width at half maximum (FWHM) of the prominent spectral lines are given in Table 2.

We found [O I] λ6300 in emission in PDS 11B (Figure 4). This line is often seen in the collimated jets driven by accreting T Tauri stars (e.g., Hartigan et al. 1995; Hartmann 2009). Whitelock et al. (1995) also noticed [O I] λ6300 in the spectrum of PDS 11B. This emission line is not seen in the spectrum of PDS 11A, both in our observations and that of Whitelock et al. (1995). Zuckerman et al. (2014) have suggested that [O I] λ6300 is formed by the photodissociation of OH molecules in the disk by far-ultraviolet stellar photons. We find evidence for the presence of He I λ4471 and λ5876 in emission in the spectra of PDS 11B (Figure 3). He I λ4471 is redshifted by 3 Å, as seen from the spectra observed on 2016 February 13. This feature was absent during the observation on March 15. He I λ5876 is affected by molecular absorption bands. However, when compared with the spectrum of PDS 11A, where He I λ5876 is equally affected by molecular band absorption, an emission component is seen at λ5876. It may be noted that Whitelock et al. (1995) identified He I λ5876 emission in PDS 11B. It is possible that He I emission lines are formed from photoionization and subsequent recombination in the accretion shock region, close to the stellar surface (Zuckerman et al. 2014). Hence, the presence of [O I] λ6300 and He I emission lines in the spectrum of PDS 11B suggest that it belongs to the class of accreting T Tauri stars.

The flux calibrated *Y*, *J*, *H*, and *K* spectra of PDS 11A and PDS 11B, normalized to band center values are shown in Figure 5. Since the signal-to-noise (S/N) is low, the spectra is smoothed to five points for display purpose. Paβ is the only prominent spectral line found in PDS 11A, which is present in emission with an EW of 3 Å. No prominent emission or absorption features are present in PDS 11B.

3.2. Spectral Type Estimation

We estimated the spectral type of PDS 11A and PDS 11B using TiO bands, the dominant molecular absorption band in M-type stars. The spectral type has been estimated from the TiO5 spectral index, which is defined as the ratio of mean flux value in 7126–7135 Å region to that at 7042–7046 Å wavelength region (Reid et al. 1995). Reid et al. (1995) derived a relation between the spectral type (SpT) and TiO5 index, SpT $= -10.775 \times$ TiO5 $+$ 8.2. They suggested using this relation as a reliable spectral type estimator in the range K7 to M6.5 dwarfs. We measured the flux values from the flux calibrated spectra obtained on 2016 February 13 and found TiO5 to be 0.60 ± 0.01 for PDS 11A and 0.56 ± 0.01 for PDS 11B. The spectral type is estimated from the above mentioned relation whereby PDS 11A is found to be M1.7 $\pm$ 0.1 and PDS 11B to be M2.1 $\pm$ 0.1. Because fractional subtypes are not used for analysis, we will be approximating the

Table 1
Journal of Spectroscopic Observations

Object	Date	Optical		Infrared			
		Exp.time (s)		Exp.time (s)			
		Gr7/1671	Gr8/1671	*Y*	*J*	*H*	*K*
(1)	(2)	(3)	(4)	(5)	(6)	(7)	(8)
PDS 11A	2016 Feb 13	1800	1800	…	…	…	…
	2016 Feb 14	…	…	1000	1000	1000	1000
	2016 Mar 15	1800	1800	…	…	…	…
PDS 11B	2016 Feb 13	1800	1800	…	…	…	…
	2016 Feb 14	…	…	1000	1000	1000	900
	2016 Mar 15	900	900	…	…	…	…
Feige 34	2016 Feb 13	600	600	…	…	…	…
HIP 34768	2016 Feb 14	…	…	400	400	240	160

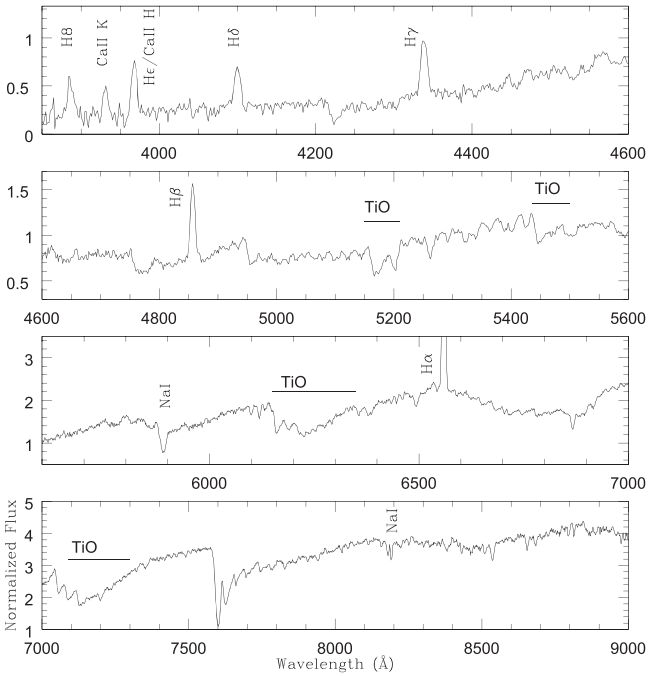

Figure 2. Optical spectrum of PDS 11A. The spectrum is flux calibrated and is normalized at 5500 Å. Prominent spectral lines are marked.

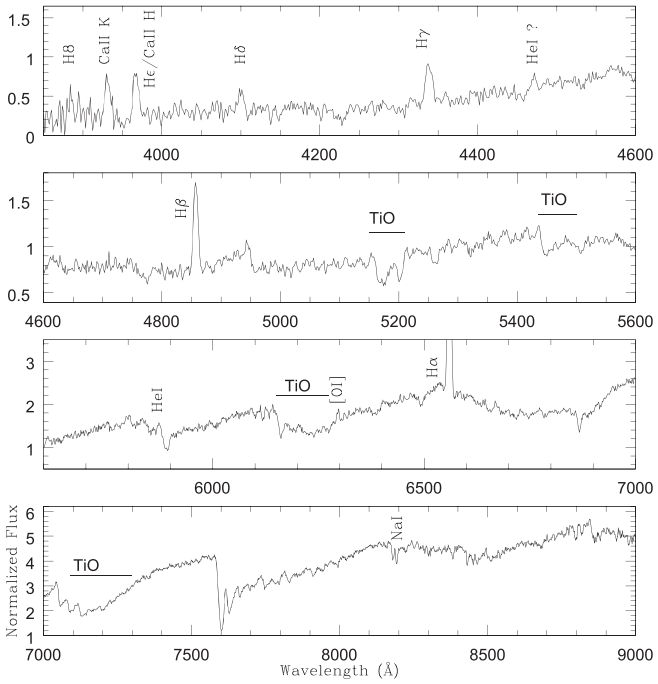

Figure 3. Optical spectrum of PDS 11B. The spectrum is flux calibrated and is normalized at 5500 Å. Prominent spectral lines are marked.

spectral type of both stars as M2, but suggest that PDS 11A can be earlier than PDS 11B by a fractional subtype. Furthermore, we compared the absorption strength of TiO λ6180 absorption feature with the M2V spectral template from Pickles library (Pickles 1998, see Figure 4). A close match between the TiO band strength of the object and the template spectrum support the M2 classification of PDS 11A and PDS 11B. The early M-type classification is further supported by the absence of TiO λ8465 band in our spectra. This band starts appearing in the spectra from M3 onward and is used as a criteria to classify objects with spectral type M3–L3 (Slesnick et al. 2006).

3.3. Hα: Accretion Indicator

Historically, the strength of the Hα line has been used to distinguish between accreting classical T Tauri stars (CTTS) from weak-lined T Tauri stars (WTTS), where the Hα emission is due to chromospheric activity. An Hα equivalent width EW(Hα) $\sim$ 10 Å was set as the discrimination boundary. However, because of the "contrast effect" of the photosphere, no unique EW(Hα) value distinguishes all CTTSs from WTTSs, and several authors have proposed EW(Hα) dividing line as function of spectral type (Martín 1998; Barrado y Navascués & Martín 2003; White & Basri 2003). White & Basri (2003) prescribed empirically determined maximum EW(Hα) values observed for non-accreting T Tauri stars for different spectral type ranges. Barrado y Navascués & Martín (2003) proposed EW(Hα) values as a function of spectral type derived from the observed saturation limit for the chromospheric activity at $\mathrm{Log}(L_{\mathrm{H}\alpha}/L_{\mathrm{bol}}) = -3.3$. Figure 6 shows both White & Basri (2003) and Barrado y Navascués & Martín (2003) criteria to distinguish between CTTSs from WTTSs. Also shown in the figure are the EW(Hα) values of PDS 11A and PDS 11B, which are well above the lines depicting White & Basri (2003) and Barrado y Navascués & Martín (2003) criteria. Thus, both PDS 11A and PDS 11B are accreting and are CTTSs.

We computed the accretion rates for PDS 11A from the Hα and Hβ line luminosities using the empirical relations given by Herczeg & Hillenbrand (2008), Fang et al. (2009), and Ingleby et al. (2013). For the distance range listed in Table 3 (114–131 pc)

Table 2
EW and FWHM of the Major Spectral Lines in PDS 11A and PDS 11B

Spectral Line	Date of Obs.	PDS 11A		PDS 11B	
		EW (Å)	FWHM (Å)	EW (Å)	FWHM (Å)
(1)	(2)	(3)	(4)	(5)	(6)
CaII K	2016 Feb 13	−23 ± 0.3	7.9 ± 0.1	−48 ± 4	8.6 ± 0.6
	2016 Mar 15	−28 ± 3	9.5 ± 1	−38 ± 6	7.5 ± 2
CaII H + Hϵ	2016 Feb 13	−22 ± 1	7.9 ± 0.4	−23 ± 3	7.8 ± 0.2
	2016 Mar 15	−17 ± 2	7.6 ± 0.3	−24 ± 4	8.0 ± 1
Hδ	2016 Feb 13	−14.6 ± 0.6	9.0 ± 0.3	−9.4 ± 0.8	9.0 ± 0.4
	2016 Mar 15	−9.1 ± 0.6	8.4 ± 0.6	−10 ± 3	8.0 ± 2
Hγ	2016 Feb 13	−12.8 ± 0.5	8.9 ± 0.2	−10.8 ± 0.6	9.3 ± 0.2
	2016 Mar 15	−11.4 ± 0.4	9.0 ± 1	−11 ± 2	8.5 ± 1
4474 (HeI?)	2016 Feb 13	...	...	−2.4 ± 0.1	6.2 ± 0.3
	2016 Mar 15	...	...	...	...
Hβ	2016 Feb 13	−10.8 ± 0.8	8.8 ± 0.4	−13.0 ± 0.7	8.6 ± 0.4
	2016 Mar 15	−7.8 ± 0.6	8.3 ± 0.3	−10 ± 1	8.4 ± 0.4
HeI 5876	2016 Feb 13	...	...	−1.9 ± 0.1	9.0 ± 0.1
	2016 Mar 15	...	...	−1.4 ± 0.4	8.2 ± 0.6
NaI (5890+5896)	2016 Feb 13	5.2 ± 0.2	12.4 ± 0.3	3.4 ± 0.2	12.7 ± 0.4
	2016 Mar 15	6.0 ± 0.2	13.5 ± 0.5	3.2 ± 0.3	13.8 ± 0.5
[O I]6300	2016 Feb 13	...	...	−1.2 ± 0.1	6.5 ± 0.1
	2016 Mar 15	...	...	−1.7 ± 0.3	5.9 ± 0.4
Hα	2016 Feb 13	−23.0 ± 0.8	7.6 ± 0.1	−27.0 ± 0.7	7.9 ± 0.2
	2016 Mar 15	−25.0 ± 0.5	7.7 ± 0.2	−25.0 ± 0.5	8.3 ± 0.2
LiI 6708	2016 Feb 13	0.45 ± 0.05	5.2 ± 0.1	...	...
	2016 Mar 15	0.40 ± 0.04	5.0 ± 0.3	...	...
NaI 8183	2016 Feb 13	0.8 ± 0.1	6.8 ± 0.2	0.8 ± 0.1	6.3 ± 0.1
	2016 Mar 15	1.0 ± 0.1	7.9 ± 0.2	0.9 ± 0.2	7.3 ± 0.2
NaI 8195	2016 Feb 13	1.0 ± 0.1	6.4 ± 0.2	1.0 ± 0.1	6.8 ± 0.1
	2016 Mar 15	1.3 ± 0.1	7.1 ± 0.1	1.1 ± 0.2	7.2 ± 0.2

Note. EW of emission lines are shown in negative.

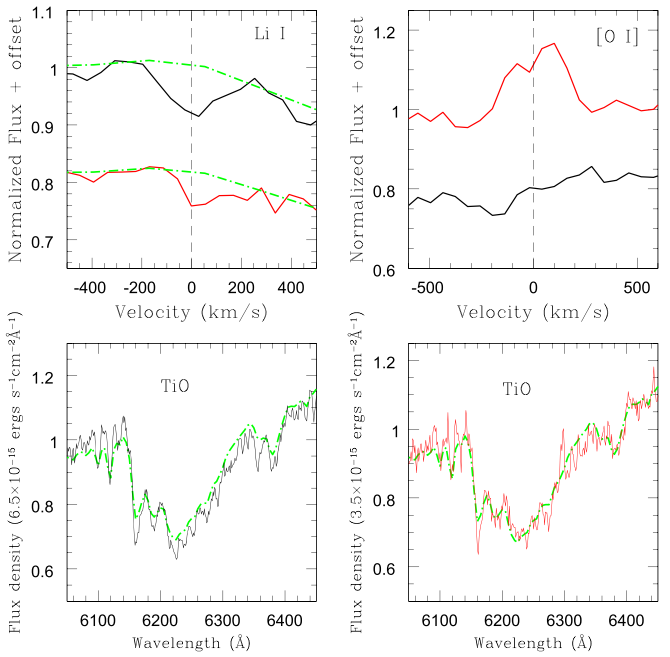

Figure 4. Li I λ6708 and [O I] λ6300 line profiles of PDS 11A and PDS 11B (red) are shown in the upper panel. The lower panel shows the TiO λ6180 band of PDS 11A (left) and PDS 11B (right). Overplotted is the M2V template from Pickles stellar library in green.

corresponding to the age range of 10–15 Myr, the accretion rates obtained are in the range of 4.2×10^{-11}–$5.0 \times 10^{-10}\,M_{\odot}\,\mathrm{yr}^{-1}$ with a median value of $\sim 1.0 \times 10^{-10}\,M_{\odot}\,\mathrm{yr}^{-1}$. The accretion rates we obtain for PDS 11A is significantly lower than that found for <3 Myr old CTTSs of spectral type M2 (e.g., Ingleby et al. 2013; Kim et al. 2016). They are, however, quite similar to the accretion rates found for M2 members of the 10–15 Myr old moving groups (e.g., Zuckerman et al. 2014). The HI line luminosity and the $L_{\rm acc}$ estimated from them for the PDS 11A are significantly higher than that expected from chromospheric activity. Following Manara et al. (2013), the noise introduced in the estimated $L_{\rm acc}$ due to chromospheric contamination (see Equation (2) in Manara et al. 2013) is $<1.8 \times 10^{-4}\,L_{\odot}$, while the accretion luminosity of PDS 11A is $\sim 1.4 \times 10^{-3}\,L_{\odot}$, which is ∼8 times higher, indicating that PDS 11A is accreting material from the disk.

From the accretion rates of PDS 11A, we further estimated the expected line flux and equivalent widths for Paβ and Brγ lines using the empirical relations from Muzerolle et al. (1998), Calvet et al. (2004) and Natta et al. (2006). For PDS 11A, the expected Paβ EW is ∼2 Å (line flux $\sim 2.1 \times 10^{-21}\,\mathrm{W\,cm^{-2}}$) and the expected Brγ EW is ∼0.3 Å (line flux $\sim 3.1 \times 10^{-22}\,\mathrm{W\,cm^{-2}}$). From the observed spectra discussed in Section 3.1, we found that Paβ EW is around 3 Å, whereas no clear emission is present in Brγ, which agrees with these estimates. Thus, the strength of the observed H I lines in the optical and near-IR spectra of PDS 11A is consistent with the star accreting at a rate of $\sim 10^{-10}\,M_{\odot}\,\mathrm{yr}^{-1}$.

3.4. Age Estimation of PDS 11A from Li I λ6708 EW

The Li I λ6708 absorption feature is an indicator of youth and is often used as one of the criteria to classify the source as a

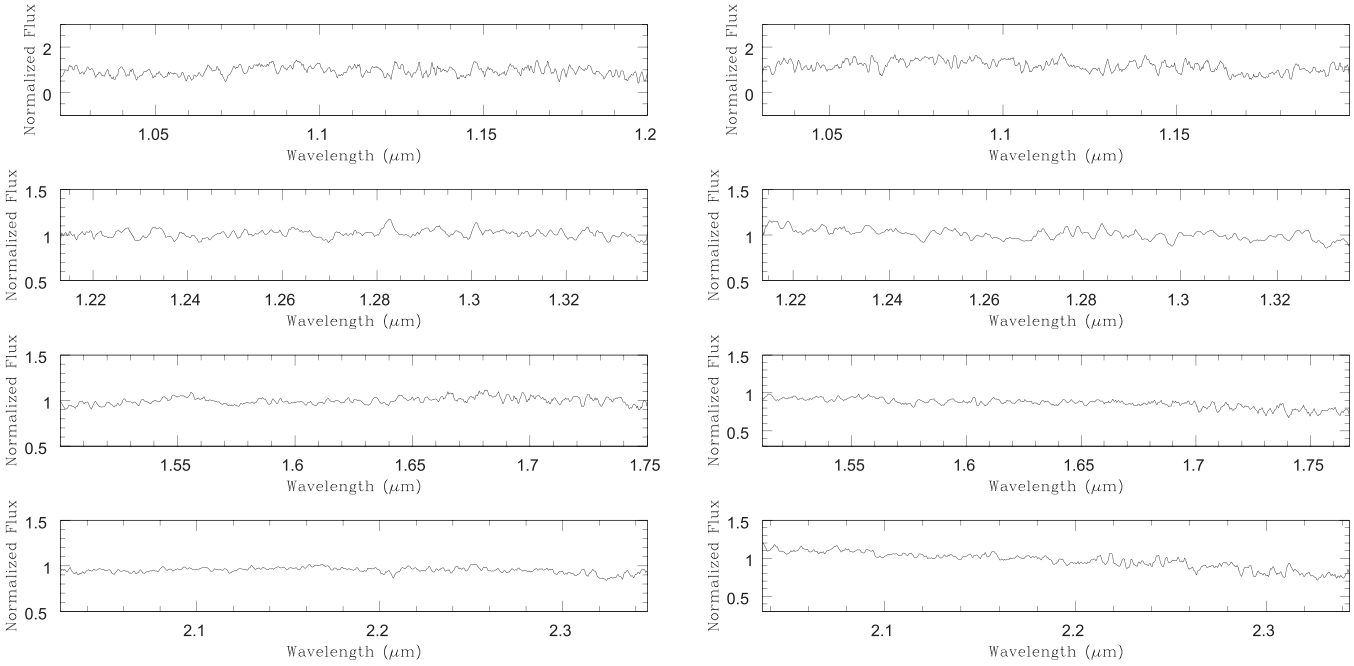

Figure 5. Near-Infrared *Y*, *J*, *H*, and *K*, spectra of PDS 11A (left) and PDS 11B (right).

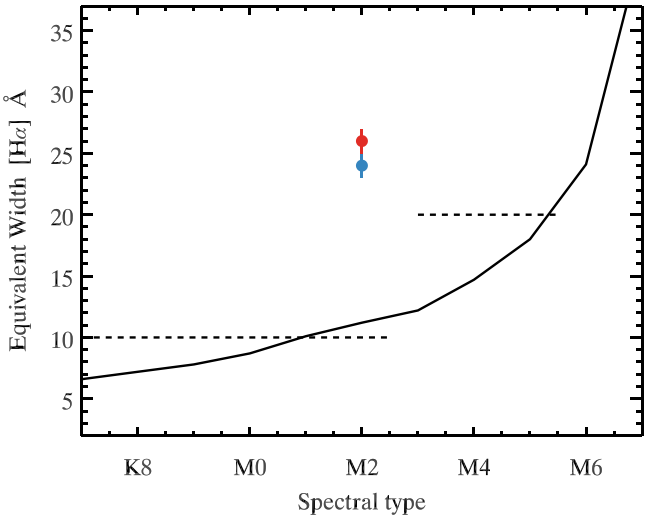

Figure 6. The EW(Hα) criterion that distinguishes CTTSs from WTTSs as a function of spectral type from White & Basri (2003) (dashed lines) and Barrado y Navascués & Martín (2003) (solid line) is shown. Observed EW(Hα) values of PDS 11A (blue solid circle) and PDS 11B (red solid circle) from 2016 February 13 are also shown.

Table 3
Stellar Properties

Reference (1)	PDS 11A (2)	PDS 11B (3)
Sp.type	M1.7 ± 0.1	M2.1 ± 0.1
$T_{\rm eff}$ (K)	3490	3490
$L_{\rm bol}$ ($L_\odot$)	0.067–0.089	⋯
$E(B-V)$	0	0
Distance (pc)	114–131	⋯
Age (Myr)	10–15	⋯
Mass ($M_\odot$)	0.4	⋯
V_r (km s^{-1})	21 ± 3(1)	10 ± 8(2)
μ_α(3) (mas yr^{-1})	6.0 ± 4.3	5.7 ± 3.4
μ_δ(3) (mas yr^{-1})	−1.4 ± 4.8	4.6 ± 2.5

References. (1) Gregorio-Hetem et al. 1992; (2) Whitelock et al.1995; (3) Qi et al. 2015.

T Tauri star (Bodenheimer 1965; Hamann & Persson 1992; Sergison et al. 2013). We found evidence for the presence of Li I λ6708 line in the spectrum of PDS 11A, with an EW of 0.43 Å (mean value of both epochs, Table 2). In Figure 4, the presence of Li I λ6708 absorption is particularly evident from the comparison of line profile with that of M2V spectral template from Pickles library. It may be noted that a tentative detection of Li I λ6708 in PDS 11B is seen in Figure 4, when compared with the template spectrum, but it can only be confirmed from spectra with better resolution and S/N. Henceforth, we will be considering Li I λ6708 absorption only in PDS 11A. Gregorio-Hetem et al. (1992) also have reported Li I λ6708 absorption line in the spectrum of PDS 11A with an EW of 0.71 Å. The identification of Li I λ6708 in the spectra of PDS 11A supports its T Tauri membership.

We used the lithium depletion boundary (LDB) technique to estimate the age of PDS 11A. This method is model independent when compared with the age estimation from stellar evolutionary models and it is often used for precise age estimation of young stars in moving groups (Soderblom 2010; Song et al. 2002; Binks & Jeffries 2014). From the measured Li I λ6708 EW, it is possible to estimate the age of the T Tauri star using LDB technique. Because we know the spectral type of our object of interest, it is possible to set an age limit during which Li I λ6708 absorption line is present in the spectra. The stellar models of Baraffe et al. (2015) show that the surface lithium is depleted in M2 stars such as PDS 11A (whose effective temperature ($T_{\rm eff}$) is 3490 K; Pecaut & Mamajek 2013) at an age of 15 Myr. This means that because Li I λ6708 is present in PDS 11A, the age should be less than 15 Myr.

To see whether the age of PDS 11A matches with young stars in moving groups, we analyzed the Li I λ6708 EW

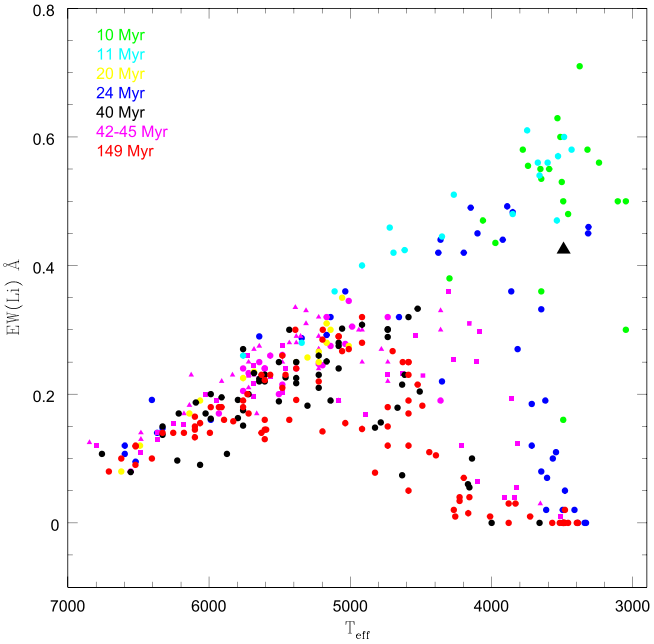

Figure 7. Liλ 6708 EW of members of various moving groups is shown as a function of their effective temperature (taken from da Silva et al. 2009). PDS 11A is shown as black triangle. The members of various groups are color coded based on their ages; TW Hya (10 Myr, green), βPic (24 Myr, blue), Tucana (45 Myr, magenta), Columba (42 Myr, magenta), Carina (45 Myr, magenta), ϵCha (11 Myr, cyan), Octans (20 Myr, yellow), Argus (40 Myr, black), and AB Dor (149 Myr, red). The ages of each of the moving groups is taken from the recent compilation by Bell et al. (2015). The age of Argus and Octans association is not listed in Bell et al. (2015), hence we used the age given in da Silva et al. (2009).

measurements of all the known members of the nine nearby moving groups identified so far, from da Silva et al. (2009). We used those values along with the stellar effective temperature (as given in da Silva et al. 2009) to analyze the Li I λ6708 EW variation with temperature (Figure 7). In Figure 7, PDS 11A is located between 10 Myr old TW Hya association and 24 Myr old β Pic moving group. It may be noted that there are no moving groups with Li I EW measurements of stars between 10 and 24 Myr. Hence, from LDB method and the analysis of Li I EW distribution in moving groups, we found that PDS 11A has an age of 10–15 Myr, which will be used in further discussion.

PDS 11 is not the first case of a T Tauri binary system where only one of the components show Li I λ6708 absorption. Song et al. (2002) found that Li I λ6708 absorption feature is seen in the secondary of the HIP 112312 (GJ 871.1 A and B) pre-MS binary system whereas it is absent in the primary. They used this system, which is about 12 Myr old and at a distance of 24 pc, to study the LDB in pre-main sequence stars. The spectral type of GJ 871.1 A and B (M4 and M4.5) is closer to that of PDS 11A and PDS 11B (M2). It is intriguing to see why Li I λ6708 is present in absorption only in one component of the binary system if they are of similar age. We note that presence of Li I λ6708 in absorption is not a necessary condition to classify the object as a T Tauri star. Baraffe & Chabrier (2010) cautioned that lithium may not always be a reliable age indicator since the lithium abundance depends on the accretion history of the star. Episodic accretion in young stars can increase the central temperature due to which lithium can get severely depleted (Chabrier et al. 1996).

3.5. Stellar Parameters

From our photometry, we estimated V and $(B-V)$ values of PDS 11A and PDS 11B as 14.75 ± 0.03 (m_{V1}), 1.43 ± 0.05, and 14.98 ± 0.03 (m_{V2}), and 1.28 ± 0.05, respectively. The intrinsic $(B-V)$ color of PDS 11A and PDS 11B is 1.46, considering that both are M2 stars (Pecaut & Mamajek 2013). Our observed $(B-V)$ colors are found to be bluer by 0.03 mag and 0.18 mag than the intrinsic values, for PDS 11A and PDS 11B, respectively. This has been noticed in previous studies and could be caused by the lower gravity of pre-MS stars with respect to the dwarfs (Song et al. 2002). From the observed $(B-V)$ values, the color excess $E(B-V)$ of both the stars is found to be negative, hence it will be considered as zero from now on. This is understandable, as these are high Galactic latitude objects and hence suffer little extinction.

Comparison with 10–15 Myr isochrones from Baraffe et al. (2015) for an M2 star ($T_{\rm eff}$ = 3490 K) indicates a mass of 0.4 $M_{\odot}$ and luminosity in the range 0.089–0.067 $L_{\odot}$ (log $L/L_{\odot} = -1.05$ to -1.17) for PDS 11A. These luminosity values imply bolometric magnitude $M_{\rm bol}$ in the range of 7.37–7.67, from which absolute V magnitude (M_{V1}) is obtained using the bolometric correction of -1.80 for M2 stars given in Pecaut & Mamajek (2013). The observed V magnitude, $m_{V1} = 14.75$, and M_{V1} indicate a distance of 114–131 pc for PDS 11A. The estimated stellar parameters are given in Table 3. Similar estimates are not possible for PDS 11B, as Li I λ6708 is not present in the spectra.

3.6. Infrared Excess

Infrared excess in the energy distribution is one of the defining criteria to identify T Tauri stars among the sample of low-mass stars (Calvet & Gullbring 1998; Meyer et al. 1997). We made use of the archival 2MASS data to estimate the near-IR $(J-H)$, $(H-K)$ colors and use them to assess near-IR excess in PDS 11A and PDS 11B. Figure 8 shows the location of PDS 11A and 11B in the $(J-H)-(H-K)$ color–color diagram. For assessing the nature of near-IR excess in PDS 11 components, we also show CTTS, WTTS, and transitional disk candidates in the figure. The 32 CTTS shown are of spectral types M0–M3 from the Taurus star-forming region, identified from Furlan et al. (2006) and Furlan et al. (2011). Also, included are 14 WTTS in the spectral type range M0–M3 from the Taurus and Chamaeleon star-forming regions (Furlan et al. 2011; Manoj et al. 2011). We have used the 2MASS colors of a sample of 16 TD candidates in Taurus and Chamaeleon I, taken from Kim et al. (2013). It is immediately evident from Figure 8 that PDS 11B shows considerable IR excess and is found to be on the CTTS locus. The $(J-H)_0$, $(H-K)_0$ colors of the object seems to be higher than the sample of CTTS used for this analysis. However, because the location do not contain T Tauri stars other than CTTS, it is pretty clear that PDS 11B belong to CTTS category. The near-IR excess of PDS 11A is similar to the WTTS/TDs, suggesting significantly less hot dust material around it. To see whether our stars have any analogs in any of the moving group in terms of near-IR colors, we represented them in a $(J-H)$ versus $(H-K)$ color–color diagram. We included stars in the spectral range M0–M3 from known moving groups listed in Zuckerman & Song (2004) and Torres et al. (2008). As seen from Figure 9, almost all of the members of various moving groups are found to be clustered near the main sequence, similar to PDS 11A. The extreme type

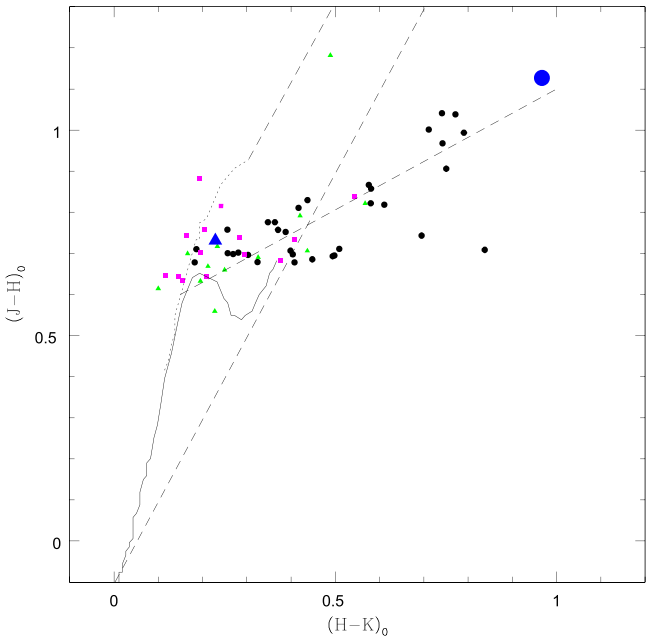

Figure 8. 2MASS $(J-H)_0$ vs. $(H-K)_0$ color–color diagram: PDS 11A and PDS 11B are shown in an open blue triangle and a circle, respectively. The sample of CTTS are shown in black circles, WTTS in magenta squares, and TD candidates in green diamonds. Main sequence and giant sequence, shown in solid and dotted lines, respectively, is from Koornneef (1983), which is converted to 2MASS system using the transformation relations from Carpenter (2001). The CTTS location is from Meyer et al. (1997) and is shown in dotted-long dash line. The $(J-H)$, $(H-K)$ colors are reddening corrected using the relation from Rieke & Lebofsky (1985).

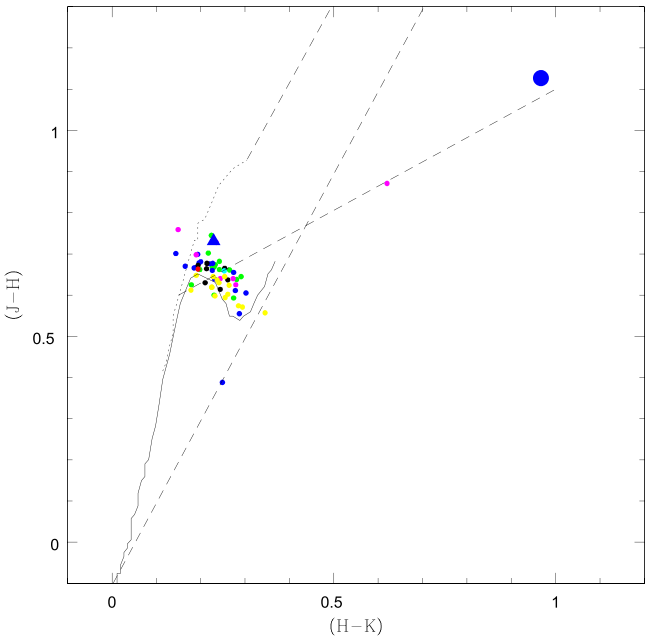

Figure 9. 2MASS $(J-H)$ vs. $(H-K)$ color–color diagram: PDS 11A and PDS 11B are shown in an open blue triangle and a circle, respectively. The sample of stars from moving groups are shown in different colored filled circles; TW Hya (green), β Pic (blue), Tucana (black), Columba (cyan), ϵ Cha (magenta), Argus (red), and AB Dor (yellow). $(J-H)$ and $(H-K)$ colors are not de-reddened since color excess values of moving groups are not available. All the other sequences are same as in Figure 8.

of IR excess seen in PDS 11B is generally not seen in any other association members. In summary, both PDS 11A and PDS 11B are found to lie on the CTTS locus, indicating the presence of warm circumstellar dust around them. In addition to the near-IR excess, both stars are accreting (Section 3.3) and show veiling in the observed spectra (discussed in Section 4.1), qualifying them as classical T Tauri stars. PDS 11B show very high near-IR excess and lies at the extreme end of the CTTS locus. Because none of the known CTTS display such high near-IR excess (see Figure 8), it is worth exploring the nature of PDS 11B from further studies.

3.7. Spectral Energy Distribution

The spectral energy distribution (SED) of PDS 11A and PDS 11B is constructed with the available photometric data given in Table 4. The SEDs are shown in Figure 10. We have used BT-Settl model atmospheres corresponding to the temperature ($T_{\rm eff}$) and gravity (log g) values of of PDS 11A and PDS 11B. Even though $T_{\rm eff}$ of both the stars are 3490 K, we have taken the BT-Settl atmosphere for 3500 K, which is the closest temperature for which stellar atmosphere is available. Generally, in the case of pre-MS stars, model atmospheres corresponding to $\log(g) = 4.5$ is used for SED analysis. We verified this in the case of PDS 11A, which has a $\log(g)$ value of 4.34 from the stellar models of Baraffe et al. (2015). Because BT-Settl model atmospheres corresponding to $T_{\rm eff} = 3490$ K and $\log(g) = 4.34$ are unavailable, we used the nearest combination of $T_{\rm eff} = 3500$ K and $\log(g) = 4.5$ for SED analysis.

PDS 11A does not show much of IR excess whereas PDS 11B shows considerable excess with the SED rising in near-IR

Table 4
Available Data

Reference (1)	Band (2)	PDS 11A (3)	PDS 11B (4)
This work	B	16.18 ± 0.04	16.27 ± 0.04
	V	14.75 ± 0.03	14.98 ± 0.03
	R	13.69 ± 0.03	13.98 ± 0.03
G92	B	16.27	16.68
	V	14.76	15.34
	R	13.70	14.28
	I	12.55	13.09
DENIS	I	12.433 ± 0.03	12.915 ± 0.03
	J	11.159 ± 0.06	11.361 ± 0.06
	K	10.259 ± 0.06	9.293 ± 0.06
2MASS	J	11.182 ± 0.026	11.332 ± 0.029
	H	10.451 ± 0.026	10.205 ± 0.029
	K	10.222 ± 0.019	9.238 ± 0.021
W95	J	11.152 ± 0.036	10.919 ± 0.189
	H	10.422 ± 0.047	9.781 ± 0.174
	K	10.185 ± 0.039	8.923 ± 0.173
	L	9.960 ± 0.061	7.872 ± 0.125

References. DENIS: DENIS Consortium 2005; 2MASS: Cutri et al. (2003); G92: Gregorio-Hetem et al. (1992); W95: Whitelock et al. (1995). L mag given in SAAO system.

itself (Figure 10). We found that mid-infrared magnitudes are available from *WISE* mission for PDS 11B, but the beam size includes PDS 11A as well. Comparison of J, H, K magnitudes of both stars from 2MASS and Whitelock et al. (1995) indicate that most of the excess emission is coming from PDS 11B. PDS 11B is about 2.2 mag brighter than PDS 11A in L band (Whitelock et al. 1995). PDS 11B shows considerably high $(J-H)$ and $(H-K)$ color excess (∼1 mag), which is even

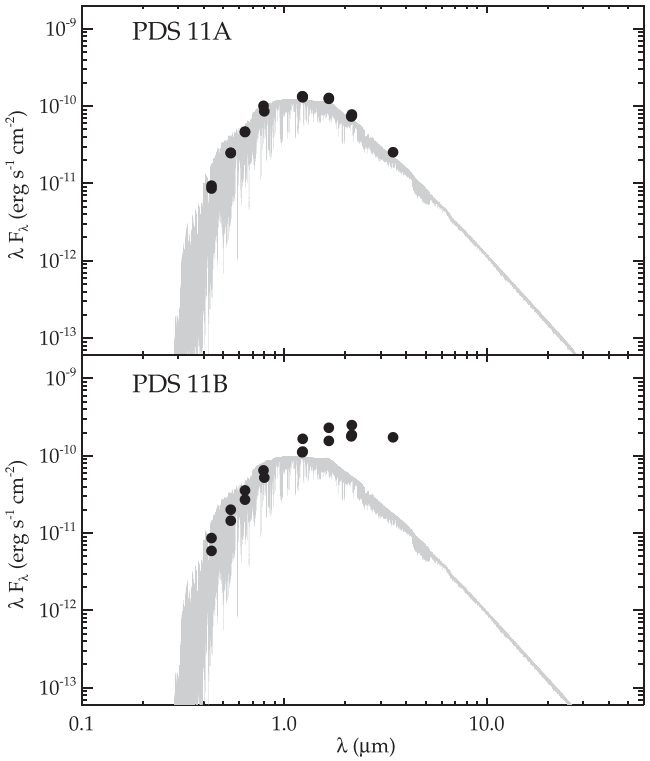

Figure 10. Observed SEDs of PDS 11A and PDS 11B. Photometry at all the epochs are plotted. For PDS 11A, they fall on top of each other, while PDS 11B show significant variability. Also shown are the BT-Settl model for $T_{\rm eff}$ = 3500 K and log(g) = 4.5. The model is normalized to the observed J-band flux.

higher than that for CTTS in star-forming region (Figure 8). We note that in addition to disk excess, the IR excess in PDS 11B can also be contributed by an unseen late-type companion, which demands further investigation.

4. Discussion

Our analysis so far suggests that both components of the PDS 11 system are of similar spectral type, M2. Both PDS 11A and PDS 11B show strong Hα emission, confirming their CTTS status. While PDS 11B shows strong excess emission in the near-IR, PDS 11A shows no or weak excess, indicating the that no hot dust is present close to the star. Intriguingly, PDS 11A shows lithium absorption, suggesting that it is 10–15 Myr old; PDS 11B does not show lithium absorption. Below we discuss more aspects on veiling and binarity of this system.

4.1. Veiling Estimate from Ca I λ4227

The presence of excess continuum emission, referred to as veiling, is often observed in classical T Tauri stars (Joy 1949; Johns-Krull & Valenti 2001). In the magnetospheric accretion model, veiling is due to the dissipation of energy in the post-shock region at the base of the magnetic funnel, close to the stellar surface (Koenigl 1991; Hartmann et al. 1994; Calvet & Gullbring 1998). Herczeg & Hillenbrand (2014) suggested a method to estimate veiling in T Tauri stars. They found that measured EW values of CaI λ4227 absorption line follow a relation with spectral type, of the form EW(Ca I) = $-189.218 + 7.36x - 0.072x^2$. Since both PDS 11A and PDS 11B are of M2 spectral type, "x" corresponds to 60 (Herczeg & Hillenbrand 2014). Hence, the expected Ca I λ4227 EW should be 6.8 Å, if veiling is not present. In the case of PDS 11A, EW(Ca I) measured on 2016 February 13 agrees with the expected value, whereas it changed to 5.6 ± 0.2 Å, when measured from the spectra taken on 2016 March 15. During the first epoch, the measured EW value of Ca I λ4227 is almost similar to that expected if veiling is not present. However, in the second epoch, the line gets veiled, suggesting that emission from accretion continuum is filling-in the absorption line. The situation is even more interesting in the case of PDS 11B, which shows a EW (Ca I) value of 6.0 ± 0.4 from the spectra taken on 2016 February 13, and the line is almost not visible in the spectra taken on 2016 March 15. Because the measured EW of Ca I λ4227 is considerably lower than the empirical estimates, PDS 11B must be undergoing strong veiling. We estimated the effect of veiling on spectral type determination for both the stars using the EW(Ca I) relation given in Herczeg & Hillenbrand (2014). We found that the spectral type of PDS 11A could change from M2 to M1 for a change in EW(Ca I) from 6.8 to 5.6 Å. In the case of PDS 11B, the Ca I λ4227 line is almost completely veiled and hence the spectral type can shift to earlier type by ∼5 subtypes.

The fact that the spectra of both the stars in PDS 11 are veiled has important implications. First, this supports our result that PDS 11A and PDS 11B are CTTS in active accretion phase. Second, this explains the absence of Li I λ6708 absorption line in PDS 11B. It is quite possible that PDS 11B is of the same age as PDS 11A and Li I λ6708 is present, but the line is filled in because of strong veiling. We examined this aspect by comparing the lithium abundance values listed in Baraffe et al. (2015) with the shift in spectral type due to veiling. In the previous paragraph, we described that veiling was present in the spectrum of PDS 11B obtained on 2016 February 13, while PDS 11A did not show evidence for veiling during that epoch. The equivalent width of Ca I λ4227 in PDS 11B was found to be 6 Å, whereas the expected value in the absence of veiling is 6.8 Å. This reduction in absorption strength due to veiling will shift the spectral type from M2 to M1 for PDS 11B, according to the EW(Ca I) relation given in Herczeg & Hillenbrand (2014). Thus, based on EW(Ca I), the spectral type of PDS 11B was of M1 and PDS 11A of M2 type for the epoch 2016 February 13. The age of PDS 11A is estimated in the range 10–15 Myr. From Baraffe et al. (2015) stellar models, it is seen that at an age of 10 Myr, the ratio of surface lithium abundance to initial abundance is ∼27 times higher in an M2 star like PDS 11A, when compared to M1 star like PDS 11B. Because we found Li I λ6708 absorption in PDS 11A to be 0.43 Å, the EW(Li I) expected for PDS 11B is around 0.02 Å. This value is far below the detection limit of our instrument, which supports our proposition that Li I λ6708 might be present in PDS 11B, but not visible in the spectrum due to strong veiling.

4.2. Possible Association with a Moving Group

We used the Banyan II webtool[7] to check whether our candidates are associated with any of the nearby kinematic groups. Banyan II is a Bayesian analysis tool which makes use of the position and space velocities of the object to assess the match with the database of nearby (<100 pc) moving groups, younger than 100 Myr (Malo et al. 2013; Gagné et al. 2014). The heliocentric radial velocity and proper motion of PDS 11A

[7] http://www.astro.umontreal.ca/~gagne/banyanII.php

and PDS 11B are taken from the literature and are given in Table 3. From the analysis, we found that PDS 11A and PDS 11B are not associated with any known moving group. Banyan II analysis gives 100% probability that PDS 11A and PDS 11B belong to young field population (Gagné et al. 2014). It is quite possible that our object parameters may not match that of any known association, hence it has been ascribed to young field population.

4.3. PDS 11: A Wide Binary Classical T Tauri System?

Although the PDS 11 system has been treated as binary in the literature (Gregorio-Hetem et al. 1992), it is yet to be demonstrated that PDS 11A and 11B are gravitationally bound. It has been identified as visual binaries in Washington Double Star catalog (Mason et al. 2001), but that does not guarantee that they are gravitationally bound. Instead, we found that the proper motion in R.A. and decl. for both stars are similar within uncertainties (Table 3). This suggests that PDS 11A and PDS 11B form a binary system. Considering PDS 11 at a distance of 114–131 pc with a separation of $8\farcs8$ between the components (Mason et al. 2001), the physical separation between PDS 11A and PDS 11B is ∼1003–1153 au. The proximity of two CTTS at such a separation argues against chance alignment and suggests that they are part of a bound system. Hence, the age and distance estimated for PDS 11A can as well be applied to PDS 11B.

From a study of T Tauri stars in Taurus-Auriga star-forming region, Bertout et al. (2007) obtained a relation to estimate the lifetime of the disk in T Tauri stars (τ_d), $\tau_d = 4 \times 10^6 (M/M_\odot)^{0.75}$, in terms of the mass of the parent star (M). Because the mass of PDS 11A and PDS 11B are estimated to be 0.4 $M_\odot$, the disk lifetime is around 2.0 Myr. Evidently, it is quite puzzling how a disk that harbors enough gas and dust survives in 10–15 Myr old system like PDS 11. T Tauri binary systems with disks at ages older than the typical disk dissipation timescales have been reported in the literature. Most of them belong to nearby (<100 pc) young moving groups. They are 8 Myr old binary systems TW Hya (Teixeira et al. 2008), HR 4796 (Kastner et al. 2008), TWA 30 (Looper et al. 2010a, 2010b), T Cha (Kastner et al. 2012), 20 Myr old V4046 Sgr (Kastner et al. 2011), and LDS 5606 (Rodriguez et al. 2014). These objects belong to a class of wide binaries, where the separation between the components is in the range 1.7 kau (for LDS 5606, Rodriguez et al. 2014) to 41 kau (for TW Hya–TWA 28 system, Teixeira et al. 2008). Among them, only TWA 30 and LDS 5606 are T Tauri binary systems in which both components are accreting. The binary components of TWA 30 system are separated by ∼3400 au, show nearly edge-on orientation and are of similar spectral type, M5 and M4, respectively (Looper et al. 2010a; Principe et al. 2016). LDS 5606 is an M5/M5 T Tauri binary system at a separation of ∼1700 au and they are members of β Pic moving group (Rodriguez et al. 2014; Zuckerman et al. 2014).

To summarize, PDS 11 is the third such system, after TWA 30 and LDS 5606, that belongs to the interesting class of old, dusty, wide binary classical T Tauri systems in which both components undergo active accretion. It is quite possible that PDS 11A is a transition disk candidate, as it is accreting and lacks hot dust material close to the star (see Sections 3.3 and 3.6). However, further studies are needed to confirm other transition disk properties such as mid- and far-IR excess and the presence of outer disk in PDS 11A. Also, further observations are needed to assess whether the near-IR excess in PDS 11B is entirely due to circumstellar material or due to the contribution from late-type companion. If confirmed, this would be the first known example of a >10 Myr old binary system where one of the components harbor a radially continuous full disk, while the other is surrounded by a disk with inner hole or gap.

5. Conclusion

We analyzed the star/disk properties and derived the spectral type of the T Tauri binary system PDS 11 from optical photometry, spectroscopy and infrared spectroscopic observations. Our analysis indicates that PDS 11 is the new addition after TWA 30 and LDS 5606 to the interesting class of old, dusty, wide binary classical T Tauri systems in which both components are actively accreting. The main conclusions from this study are listed below.

1. The spectral type of PDS 11A and PDS 11B were not known. We have classified both as M2 type making use of the TiO λ7050 band feature, with the aid of TiO5 index and the relations from Reid et al. (1995).
2. PDS 11A and PDS 11B are found to have Hα emission strength of ∼25 Å, which is higher than the threshold value of chromospherically active stars. The median accretion rate derived from Hα emission line is around $\sim 1.0 \times 10^{-10} M_\odot\,\mathrm{yr}^{-1}$ for PDS 11A. PDS 11B show very high near- and mid-infrared excess. The emission lines of [O I] λ6300 and He I λ5876, indicative of accretion process, are present in the spectrum of PDS 11B. All these evidences conclusively prove that PDS 11A and PDS 11B are classical T Tauri stars. It needs to be assessed from future studies how an active accretion disk sustains in a 10–15 Myr old system like PDS 11A.
3. We found that PDS 11A is less than 15 Myr from age dating using lithium depletion boundary method. Further, from the comparison of Li I λ6708 EW with that of young stars in moving groups, the age is constrained in the range 10–15 Myr.
4. Because Li I λ6708 is not present in the spectrum of PDS 11B, the stellar parameters other than spectral type and temperature were not determined. However, because we prove that PDS 11A and PDS 11B form a binary system, the age and distance of PDS 11B is taken to be similar to PDS 11A.
5. From our analysis, PDS 11 is identified as a binary system with component masses of 0.4 $M_\odot$, luminosity of 0.067–0.089 $L_\odot$ and at a distance of 114–131 pc.
6. From the analysis with Banyan II webtool, PDS 11A and PDS 11B were not identified as members of any known moving group and hence is considered as a young field binary system.

We thank the staff at IAO, Hanle and its remote control station at CREST, Hosakote for their help during the observation runs. This research uses the SIMBAD astronomical data base service operated at CDS, Strasbourg. This research made use data of 2MASS, which is a joint project of University of Massachusetts and the Infrared Processing and Analysis Centre/California Institute of Technology, funded by the National Aeronautics and Space Administration and the National Science Foundation.

References

Appenzeller, I., & Mundt, R. 1989, A&ARv, 1, 291
Baraffe, I., & Chabrier, G. 2010, A&A, 521, A44
Baraffe, I., Homeier, D., Allard, F., et al. 2015, A&A, 577, A42
Barrado y Navascués, D., & Martín, E. L. 2003, AJ, 126, 2997
Bell, C. P. M., Mamajek, E. E., & Naylor, T. 2015, MNRAS, 454, 593
Bertout, C. 1989, ARA&A, 27, 351
Bertout, C., Siess, L., & Cabrit, S. 2007, A&A, 473, L21
Bessell, M. S. 1990, PASP, 102, 1181
Binks, A. S., & Jeffries, R. D. 2014, MNRAS, 438, L11
Bodenheimer, P. 1965, ApJ, 142, 451
Calvet, N., & Gullbring, E. 1998, ApJ, 509, 802
Calvet, N., Muzerolle, J., Briceno, C., et al. 2004, AJ, 128, 1294
Carpenter, J. M. 2001, AJ, 121, 2851
Chabrier, G., Baraffe, I., & Plez, B. 1996, ApJL, 459, L91
Cutri, R. M., Skrutskie, M. F., van Dyk, S., et al. 2003, yCat, 2246, 0
da Silva, L., Torres, C. A. O., de La Reza, R., et al. 2009, A&A, 508, 833
de la Reza, R., Torres, C. A. O., Quast, G., et al. 1989, ApJL, 343, L61
Elliott, P., Bayo, A., Melo, C. H. F., et al. 2016, A&A, 590, A13
Fang, M., van Boekel, R., Wang, W., et al. 2009, A&A, 504, 461
Furlan, E., Hartmann, L., Calvet, N., et al. 2006, ApJS, 165, 568
Furlan, E., Luhman, K. L., Espaillat, C., et al. 2011, ApJS, 195, 3
Gagné, J., Lafreniére, D., Doyon, R., et al. 2014, ApJ, 783, 121
Gregorio-Hetem, J., Lepine, J. R. D., Quast, G. R., et al. 1992, AJ, 103, 549
Hamann, F., & Persson, S. E. 1992, ApJS, 82, 247
Hartigan, P., Edwards, S., & Ghandour, L. 1995, ApJ, 452, 736
Hartmann, L. 2009, Accretion Processes in Star Formation (2nd ed.; Cambridge: Cambridge Univ. Press)
Hartmann, L., Hewett, R., & Calvet, N. 1994, ApJ, 426, 669
Herbig, G. H. 1962, AdA&A, 1, 47
Herczeg, G. J., & Hillenbrand, L. A. 2008, ApJ, 681, 594
Herczeg, G. J., & Hillenbrand, L. A. 2014, ApJ, 786, 97
Ingleby, L., Calvet, N., Herczeg, G., et al. 2013, ApJ, 767, 112
Johns-Krull, C. M., & Valenti, J. A. 2001, ApJ, 561, 1060
Joy, A. H. 1945, ApJ, 102, 168
Joy, A. H. 1949, ApJ, 110, 424
Kastner, J. H., Sacco, G. G., Montez, R., et al. 2011, ApJL, 740, L17
Kastner, J. H., Thompson, E. A., & Montez, R. 2012, ApJL, 747, L23
Kastner, J. H., Zuckerman, B., & Bessell, M. 2008, A&A, 491, 829
Kastner, J. H., Zuckerman, B., Weintraub, D. A., et al. 1997, Sci, 277, 67
Kenyon, S. J., & Hartmann, L. 1995, ApJS, 101, 117
Kim, K. H., Watson, D. M., Manoj, P., et al. 2013, ApJ, 769, 149
Kim, K. H., Watson, D. M., Manoj, P., et al. 2016, arXiv:1604.07907
Koenigl, A. 1991, ApJL, 370, L39
Koornneef, J. 1983, A&A, 128, 84
Looper, D. L., Bochanski, J. J., Burgasser, A. J., et al. 2010a, AJ, 140, 1486
Looper, D. L., Mohanty, S., Bochanski, J. J., et al. 2010b, ApJ, 714, 45
Malo, L., Doyon, R., Lafreniére, D., et al. 2013, ApJ, 762, 88
Mamajek, E. E. 2016, in IAU, Symp. 314, Young Stars & Planets Near the Sun, ed. J. H. Kastner, B. Stelzer, & S. A. Metchev (Cambridge: Cambridge Univ. Press), 21
Manara, C. F., Beccari, G., Da Rio, N., et al. 2013, A&A, 558, A114
Manoj, P., Kim, K. H., Furlan, E., et al. 2011, ApJS, 193, 11
Martín, E. L. 1998, AJ, 115, 351
Mason, B. D., Wycoff, G. L., Hartkopf, W. I., et al. 2001, AJ, 122, 3466
McGehee, P. M. 2008, in Handbook of Star-forming Regions, Vol. II: The Southern Sky ASP Monograph Publications, Vol. 5, ed. B. Reipurth (San Francisco, CA: ASP), 813
Meyer, M. R., Calvet, N., & Hillenbrand, L. A. 1997, AJ, 114, 288
Muzerolle, J., Calvet, N., & Hartmann, L. 1998, ApJ, 492, 743
Natta, A., Testi, L., & Randich, S. 2006, A&A, 452, 245
Ninan, J. P., Ojha, D. K., Ghosh, S. K., et al. 2014, JAI, 3, 1450006
Pecaut, M. J., & Mamajek, E. E. 2013, ApJS, 208, 9
Pickles, A. J. 1998, PASP, 110, 863
Principe, D. A., Sacco, G., Kastner, J. H., et al. 2016, MNRAS, 459, 2097
Qi, Z., Yu, Y., Bucciarelli, B., et al. 2015, AJ, 150, 137
Reid, I. N., Hawley, S. L., & Gizis, J. E. 1995, AJ, 110, 1838
Rieke, G. H., & Lebofsky, M. J. 1985, ApJ, 288, 618
Rodriguez, D. R., Zuckerman, B., Faherty, J. K., et al. 2014, A&A, 567, A20
Rucinski, S. M., & Krautter, J. 1983, A&A, 121, 217
Sergison, D. J., Mayne, N. J., Naylor, T., et al. 2013, MNRAS, 434, 966
Slesnick, C. L., Carpenter, J. M., Hillenbrand, L. A., et al. 2006, AJ, 132, 2665
Soderblom, D. R. 2010, ARA&A, 48, 581
Song, I., Bessell, M. S., & Zuckerman, B. 2002, ApJL, 581, L43
Tachihara, K., Neuhäuser, R., & Fukui, Y. 2009, PASJ, 61, 585
Teixeira, R., Ducourant, C., Chauvin, G., et al. 2008, A&A, 489, 825
Torres, C. A. O., Quast, G. R., Melo, C. H. F., & Sterzik, M. F. 2008, in Handbook of Star-forming Regions, Vol. II: The Southern Sky ASP Monograph Publications, Vol. 5, ed. B. Reipurth (San Francisco, CA: ASP), 757
White, R. J., & Basri, G. 2003, ApJ, 582, 1109
Whitelock, P., Menzies, J., Feast, M., et al. 1995, MNRAS, 276, 219
Zuckerman, B., & Song, I. 2004, ARA&A, 42, 685
Zuckerman, B., Vican, L., & Rodriguez, D. R. 2014, ApJ, 788, 102